Bioactive Materials 6 (2021) 1699–1710

Contents lists available at ScienceDirect

Bioactive Materials

journal homepage: www.sciencedirect.com/journal/bioactive-materials

The development of laminin-alginate microspheres encapsulated with Ginsenoside Rg1 and ADSCs for breast reconstruction after lumpectomy

I-Hsuan Yang [a], Yo-Shen Chen [b,**], Jia-Jing Li [b], Ya-Jyun Liang [a], Tzu-Chieh Lin [a], Subhaini Jakfar [a], Minal Thacker [a], Shinn-Chih Wu [c], Feng-Huei Lin [a,d,*]

[a] Department of Biomedical Engineering, College of Medicine and College of Engineering, National Taiwan University, No. 49, Fanglan Rd, Taipei, 10672, Taiwan
[b] Division of Plastic Surgery, Department of Surgery, Far Eastern Memorial Hospital, No. 21, Sec. 2, Nanya S. Rd., New Taipei City, 220, Taiwan
[c] Department of Animal Science and Technology, National Taiwan University, No. 1, Section 4, Roosevelt Road, Taipei City, 10617, Taiwan
[d] Institute of Biomedical Engineering and Nanomedicine, National Health Research Institutes, No. 35, Keyan Road, Zhunan, Miaoli County, 35053, Taiwan

ARTICLE INFO

Keywords:
Laminin-alginate microspheres
Adipose-derived stem cells
Ginsenoside Rg1
Bio-electrospray
Tissue engineering

ABSTRACT

Many technologies have been developed for breast reconstruction after lumpectomy. Although the technologies achieved promising success in clinical, there are still many shortages hanging over and trouble the researchers. Tissue engineering technology was introduced to plastic surgery that gave a light to lumpectomy patients in breast reconstruction. The unexpected absorption rate, resulting from limited vascularization and low cell survival rate, is a major factor that leads to unsatisfactory results for the previous studies in our lab. In the study, the laminin-modified alginate synthesized by a new method of low concertation of sodium periodate would be mixed with ADSCs and Rg1 in the medium; and then sprayed into a calcium chloride ($CaCl_2$) solution to prepare into microsphere (abbreviated as ADSC–G-LAMS) by bio-electrospray with a power syringe for the mass production and smaller bead size. The developed ADSC–G-LAMS microspheres had the diameter of 232 ± 42 μm. Sustained-release of the Rg1 retained its biological activity. WST-1, live/dead staining, and chromosome aberration assay were evaluated to confirm the safety of the microspheres. In *in vivo* study, ADSC–G-LAMS microspheres combined with autologous adipocytes were transplanted into the dorsum of rats by subcutaneous injection. The efficacy was investigated by H&E and immunofluorescence staining. The results showed that the bioactive ADSC–G-LAMS microspheres could integrate well into the host adipose tissue with an adequate rate of angiogenesis by constantly releasing Rg1 to enhance the ADSC or adipocyte survival rate to join tissue growth and repair with adipogenesis for breast reconstruction after lumpectomy.

1. Introduction

Cancer is a major disease and the second leading cause of death worldwide. Among females, the most common cancer is breast cancer. In 2019, breast cancer accounts for 30% of all new cancer diagnoses in the United States [1,2]. The most common treatment of breast cancer is breast cancer surgery, such as mastectomy or lumpectomy [3]. Because women are frequently concerned regarding aesthetics, the demand for breast reconstruction is a critical issue after surgery. In clinical practice, several methods have been developed for breast reconstruction. Silicone-based implants are the earliest and common methods for breast reconstruction. However, these implants are foreign bodies, which might induce severe foreign body reactions, such as thick fibrous encapsulation resulting in the generation of stress between an implant and the surrounding tissue. This stress may lead to capsular contraction, implant rupture and leakage, poor tactile quality, and even unnatural shape [3–5]. In the late 1970s, tissue and free flaps harvested from the abdomen, upper back, thighs, and buttocks were used as autologous tissues for breast reconstruction [6]. The limitation of a flap is the lack of enough donor sites for this procedure; moreover, complications occur in approximately 30% cases after transplantation [3,7,8]. In lipofilling technology, the fat of a patient is collected as a fat graft by liposuction and subsequently transplanted into the lumpectomy site as an autologous implant. Nowadays, lipofilling is a well-established therapy for the

* Corresponding author. Department of Biomedical Engineering, College of Medicine and College of Engineering, National Taiwan University, No. 49, Fanglan Rd, Taipei 10672, Taiwan.
** Corresponding author.
E-mail addresses: psjim01@yahoo.com.tw (Y.-S. Chen), double@ntu.edu.tw (F.-H. Lin).

https://doi.org/10.1016/j.bioactmat.2020.11.029
Received 24 September 2020; Received in revised form 2 November 2020; Accepted 27 November 2020
2452-199X/© 2020 The Authors. Production and hosting by Elsevier B.V. on behalf of KeAi Communications Co., Ltd. This is an open access article under the CC BY-NC-ND license (http://creativecommons.org/licenses/by-nc-nd/4.0/).

lumpectomy and has been combined with the scaffolds for whole breast reconstruction [9]. However, the unmet needs were owing to the unpredictable resorption rate, limited vascularization, and the calcified tissue generation occurring approximately 4–6 months post-surgery [10]. The goals of the researchers were to develop an engineered fat to maximize vascularization and minimize the resorption of the grafts.

In view of the above description, numerous technologies were developed for breast reconstruction after mastectomy or lumpectomy. Although these technologies have achieved promising success in clinical practice, there are still numerous drawbacks challenging researchers. In 1998, tissue engineering technology was introduced in plastic surgery that allowing mastectomy or lumpectomy patients to overcome the previous shortages by adipose tissue engineering for breast reconstruction [11].

The three major elements of tissue engineering are cells, scaffolds, and signals. Numerous tissue engineering technologies have been proposed for breast reconstruction; although these technologies might satisfy some of the objectives, they are still far from meeting the clinical requirements and expectations of the patient. In this study, adipose-derived stem cells (ADSCs) were used as the cell source, because ADSCs can differentiate between adipocytes, chondrocytes, myocytes, endothelial cells, and osteoblasts under specific signal induction [3,12,13]. The concept of scaffold design is the construction of a good environment for the cells towards a desired pathway. From the distinct applications in tissue engineering, the scaffolds could be formed in different forms. In recent years, the mini-invasive surgery has been developed for the augmentation. One of the scaffolds, microspheres have been used as popular carriers for several reasons. The microspheres allowed oxygen, nutrients, and waste products to exchange properly [14,15]. The cells or the bioactive materials could also be encapsulated into the microspheres as a controlled delivery system [16,17]. Numerous biodegradable materials have been used as base materials to prepare scaffolds to support cell growth and survival. Alginate is a biodegradable polymer in which cells can be encapsulated to form injectable hydrogels, beads, and preformed scaffolds [18–21]. Although there is a lack of domains for cell recognition, alginate can graft some molecules to improve cell adhesion and proliferation as well as to attain a desired differentiation [19]. Laminin, a major extracellular matrix glycoprotein, was first discovered intracellularly in the morula stage [22]. It has been shown to play an important role in early embryonic cell polarization and to effect cell differentiation, migration, and adhesion [23–25]. In this study, we used a relatively low concentration of sodium periodate ($NaIO_4$) over a long reaction time to synthesize laminin-modified alginate to prepare scaffolds for mimicking the embryonic environment.

As mentioned previously, the unexpected absorption rate, resulting from the limited vascularization and low cell survival rate, is a major factor that leads to surgery failure or unsatisfactory results. Numerous types of growth factors have been used for vascularization in tissue engineering, such as the vascular endothelial growth factor, basic fibroblast growth factor (bFGF), and platelet-derived growth factor [26,27]. However, these protein-based growth factors may not sustain a long period of biological activity. For instance, the half-life of the bFGF is approximately 50 min in the physiological environment [28]. Ginsenoside Rg1, a major component of Panax ginseng, has been reported a non-peptide bioactive molecule for mild angiogenesis with long biostability in the physiological environment [29–32].

In our previous studies, the laminin-alginate beads were prepared by the peristaltic pump with an average diameter of 1.5 mm; that was resulted in a bigger bead size to limit the diffusion of the nutrients/oxygen and then caused to the cell death in the central part of the microspheres. In the study, a bio-electrospray with a power syringe was used to prepare smaller bead sizes for better mass transportation and for mass production in the manufactory system. Furthermore, the previous studies did not add in any angiogenic factors; nonetheless, we added in Rg1 to the microsphere to induce vascularization to increase cell survival rate *in vivo* in this study. The concentration of the sodium periodate was down to 10 mM for better cell viability. Overall, in the previous studies, the bigger bead size, limited vascularization, and high concentration of sodium periodate might restrict homogeneous nutrients transportation, reduce cell survival rate *in vivo*, and biocompatibility, respectively. In this study, we develop an autologous fat graft in the form of injectable microspheres with Rg1 addition to enhance angiogenesis and cell survival rate for breast reconstruction after lumpectomy. Laminin-modified alginate was mixed with ADSCs and Rg1 in a medium, and subsequently sprayed into a calcium chloride ($CaCl_2$) solution by bio-electrospraying with a power syringe, to form microspheres (abbreviated as ADSC–G-LAMS). The ADSC–G-LAMS microspheres were collected and combined with adipocytes to produce the necessary growth factors to make the ADSCs towards the adipogenic pathway. The ADSC–G-LAMS microspheres and adipocytes were combined and prepared into an injectable form for breast reconstruction. The overall design is illustrated in Scheme 1.

2. Materials and methods

2.1. Materials

Alginic acid sodium salt (Cat. No. A2158), $NaIO_4$, and Dulbecco's modified Eagle's medium (high glucose) were purchased from Sigma-Aldrich (St. Louis, MO, USA). Fetal bovine serum (FBS) was purchased from Hyclone (Logan, Utah, USA). Natural mouse laminin (Cat. No. 354232) and Matrigel (Cat. No. 356231) were purchased from Corning (Bedford, MA, USA). Ginsenoside Rg1 was purchased from ChromaDex (Irvine, CA).

2.2. Synthesis of laminin-modified alginate

A laminin alginate solution was prepared as follows. Briefly, 0.5 mL of 10 mM $NaIO_4$ solution was added to 100 mL of 1.5% (w/v) alginate solution and stirred at room temperature in dark for 5 h before adding 0.5 mL of ethylene glycol to stop the reaction. The resultant solution was dialyzed against deionized water using a dialysis membrane (MWCO: 6000–8000 Da) for 3 days, during which time the deionized water was renewed every 12 h. The solution was lyophilized to yield the oxidized alginate powder, 1.5 g of which was dissolved in 100 mL of 20 mM 4-(2-hydroxyethyl)-1-piperazineethanesulfonic acid (HEPES). Thereafter, 10 μg of laminin was added to complete the synthesis of the laminin-modified alginate.

2.3. Preparation of laminin-modified alginate microspheres

The laminin-modified alginate microspheres were prepared by the bio-electrospray method, which is briefly described as follows. The bio-electrospray device consisted of three parts: a syringe pump, high-voltage generator, and collecting tank with 0.1 M $CaCl_2$ solution. Approximately 10 mL of the laminin-modified alginate solution was sprayed into the collecting tank with gentle stirring. The flow rate of the syringe pump was set as 0.04 mL/min with a low working voltage of 18 kV. The distance from the syringe needle to the collecting tank was 1.5 cm, and the inner diameter of the needle was 500 μm. Finally, the microspheres were washed thrice with 20 mM HEPES and collected for the subsequent experiments.

2.4. Preparation of Rg1 encapsulated in G-LAMS

As mentioned, the G-LAMS microspheres encapsulate Rg1 into the LAMS microsphere. The preparation procedure of the G-LAMS microspheres is briefly described as follows. Specifically, 10 mL of Rg1 (400 μg/mL) was added to the previously prepared LAMS (Section 2.3) and incubated at 37 °C for 24 h to allow Rg1 penetrate to the microspheres.

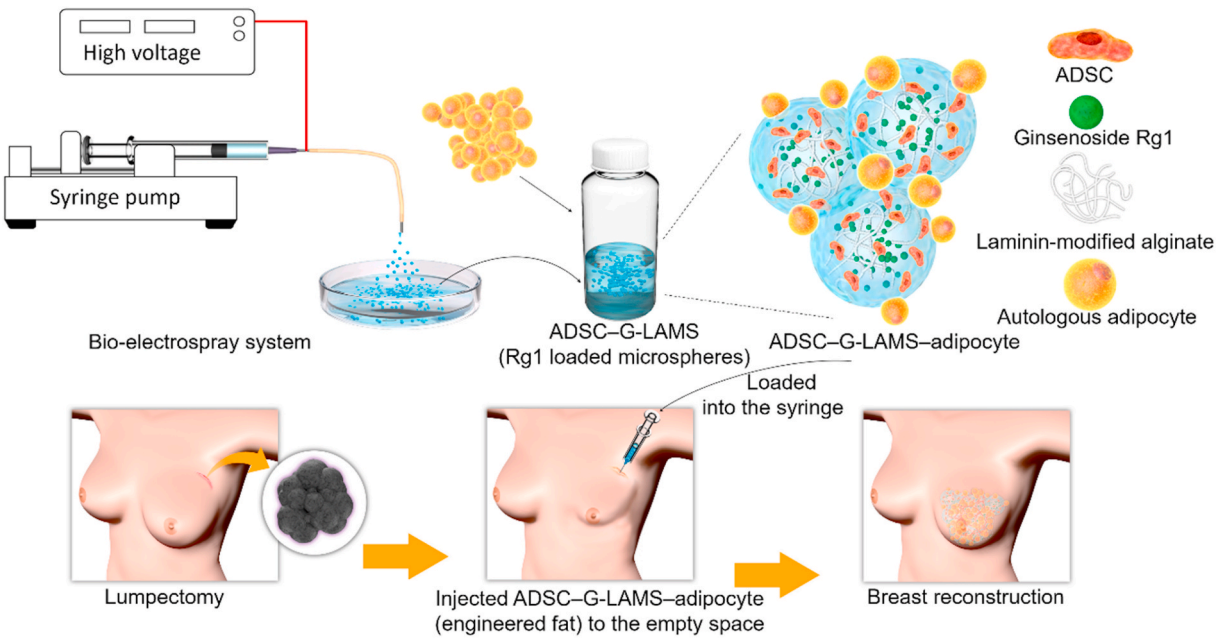

Scheme 1. The Scheme of ADSC-G-LAMS preparation and its applications for breast reconstruction.

2.5. Preparation of ADSC-G-LAMS microspheres

ADSC-G-LAMS is laminin-modified alginate mixed with ADSCs and Rg1 and converted into microspheres by bio-electrospraying, as described in Section 2.4.

The ADSCs were isolated from five-week-old female SD rats obtained from BioLASCO, Taiwan [20,33]. The inguinal fat was removed, fragmented with surgical scissors, washed with phosphate-buffered saline (PBS), and dissociated with type I collagenase (Invitrogen, USA) at 37 °C for 4 h. Following this, the samples were filtered through a 70-μm strainer and centrifuged at 1000 rpm for 5 min. The cell pellets were collected and washed twice with PBS. Subsequently, the cells were cultured in a petri dish at a density of 5000 cells/cm^2 in DMEM with 10% FBS and 1% antibiotic–antimycotic and incubated overnight at 37 °C in a humidified incubator. After 24 h, the non-adherent cells were removed and rinsed twice with PBS. The medium was changed every 3 days until confluence. The ADSCs from passages 3–5 were used for subsequent experiments.

Approximately 2 × 10^7 ADSCs were suspended in 10 mL of the laminin-modified alginate solution, and the microspheres were prepared by bio-electrospray, as described above. For the *in vivo* study, the ADSCs were isolated from green fluorescent protein transgenic (GFP) 7-week-old female SD rats. The isolated ADSCs with GFP are denoted as GFP–ADSCs.

2.6. FTIR spectrophotometry analysis

An FTIR spectrophotometer (Jasco, FT/IR-4200, Japan) was used to identify the functional groups of the laminin-modified alginate. Freeze-dried samples were mixed with KBr at a weight ratio of 1:9, and subsequently placed in an aluminium ring to form a disc by applying a gentle pressure. The FTIR patterns were obtained in transmission mode with 16 scans from 600 cm^{-1}–4000 cm^{-1}.

2.7. Size measurement and morphology observation of developed ADSC–G-LAMS microspheres

The ADSC–G-LAMS microspheres were cultured in DMEM with 10% FBS and 0.1% Primocin-antibiotic (Invivogen, San Diego, CA). The morphology of the developed ADSC–G-LAMS microspheres was observed using an optical microscope equipped with a high-intensity LED light for better brightness. The size of the developed ADSC–G-LAMS microspheres was measured by ImageJ Software images, and at least 100 ADSC–G-LAMS microspheres were counted under an optical microscope.

2.8. SEM examination of prepared ADSC–G-LAMS microspheres

At day 5 of culturing ADSC–G-LAMS in the petri dish, the ADSC–G-LAMS microspheres were washed twice with the HEPES buffer and then collected. The collected microspheres were immersed step-by-step in the dehydration series, followed by a critical point dryer (CPD). The CPD-dried microspheres were mounted on an Al stage and then coated with a platinum film by sputtering physical vapor deposition. The ADSC–G-LAMS microspheres were examined under a scanning electron microscope (S-4800, Hitachi, Japan) with 5 kV and 9000 nA for microstructure examination.

2.9. Cytotoxicity of developed G-LAMS microspheres

The cell viability of the G-LAMS microspheres was evaluated using a WST-1 assay. The G-LAMS microspheres were soaked in a medium for 24 h, and the extracts were cultured with 3T3-L1 fibroblasts for the cell viability test. 3T3-L1 cultured in DMEM was set as the control group. ZDEC extract was selected as the positive control group, Al_2O_3 extract as the negative control group. This was in terms of the cytotoxicity of the developed G-LAMS microspheres based on the ISO-10993 guideline. Each group was four repeats.

2.10. ADSC viability in developed ADSC–G-LAMS microspheres

The viability of the ADSCs in the G-LAMS microspheres was evaluated by a live/dead staining assay. At day 1 and day 5 after the ADSCs were encapsulated in the G-LAMS microspheres (ADSC–G-LAMS), the microspheres were gently washed twice and stained with dyes in dark at 37 °C for 1 h. Living and dead cells were stained with calcein AM and ethidium homodimer-1, respectively. The sample was then mounted on a glass slide and observed under a fluorescent microscope, where the living and dead cells appeared green and red in color, respectively, by the specific wavelength of the light emission.

2.11. Releasing profiles of Rg1 from G-LAMS microspheres

The releasing profiles of Rg1 from the G-LAMS microspheres were recorded by HPLC. The G-LAMS microspheres were placed in deionized water at 37 °C (n = 3) for some time and then removed for centrifugation. The supernatant was collected before injection into the HPLC system.

2.12. Tube formation ability of released Rg1

The tube formation ability of the released Rg1 was determined using HUVECs, which is regarded as the ability of angiogenesis. A 96-well plate was prior coated with 50 μL of Matrigel™. The HUVECs (1×10^4) were seeded per well in 150 μL of medium 199 (M199) containing 2% FBS and the released Rg1. The M199 with 2% FBS was used as the blank control, and M199 with 2% FBS and the endothelial cell growth supplement (ECGS, 30 μg/mL) was used as the positive control. After 6 h, images were captured using an optical microscope. The images were converted into grayscales, and the formed tube length was determined using an angiogenesis analyzer with the ImageJ software (n = 5).

2.13. Effect of G-LAMS on HUVEC gene expression

The HUVECs were seeded into a six-well plate by 1.67×10^5 cells in each well for 24 h until full adhesion and subsequently starved with M199 serum-free medium for further 4 h. The medium was then changed to 1.775 mL of M199 containing 2% FBS. The LAMS or G-LAMS microspheres were added as experimental groups. The blank medium served as the control group. After an hour of treatment, the HUVECs were collected, washed twice with PBS, and lysed with TRIzol reagent (Thermo Fisher). The supernatants were collected, and the total RNA was extracted with Direct-zol™ RNA MiniPrep Kits (Zymo Research, Irvine, CA, USA). The cDNA for real-time Q-PCR analysis was obtained by RNA reverse transcription using SuperScript™ III reverse transcriptase (Thermo Fisher). The synthesized cDNA was mixed with SYBR green master mix (Thermo Fisher). The primers used in the analysis are listed in supplemental Table S1. The intensities were detected and recorded using a LightCycler® 480 Instrument (Roche Diagnostics Nederland BV, Almere, Netherlands) (n = 3).

2.14. Evaluation of genotoxicity of G-LAMS microspheres by chromosome aberration assay

Approximately 2×10^5 of Chinese hamster ovary cells (CHO cells) were plated in a 10-cm petri dish for 20 h. Subsequently, 10 mL of the G-LAMS extract was added as the experimental group, and the culture medium only served as the control group. After 18 h of treatment, 200 μL of 10 μg/mL colchicine was added. At 20 h, the cells were trypsinized and collected in a centrifugation tube. Subsequently, 5 mL of 0.075 M KCl was added to the centrifugation tube and gently shaken. The tubes were left at 37 °C for 15 min to allow cell swelling and subsequently fixed with 5 mL of the fixation solution (methanol: acetic acid = 3:1) at 4 °C for 20 min. The suspension was dropped to a glass slide by a force to break down the cells; the breakdown cells were then stained with 10% Giemsa (Sigma) for 15 min. A total of 70 breakdown metaphase cells were counted under the optical microscope. The sister chromosome aberration was recorded. The P-value of the aberration frequency was analyzed using a one-sided Fisher's exact test.

2.15. In vivo study

A total of 12 SD rats (BioLASCO, Taiwan) with an average age of 6 weeks was used in the study. The study protocol was approved by the Institutional Animal Care and Use Committee (IACUC, No. 2018-FEMH-11) of the Far Eastern Memorial Hospital.

In *in vivo* study, the shredded adipose tissue was isolated before the materials implantation. The procedure was described below. After anesthesia, 1 mL of the inguinal fat was removed from the rat and fragmented with surgical scissors for later use. The study included three groups: (1) 2×10^6 GFP–ADSCs combined with a shredded adipose tissue. The group is abbreviated as "ADSC–adipocyte"; (2) 2×10^6 GFP–ADSCs encapsulated in 1 mL of the laminin-alginate microspheres combined with a shredded adipose tissue and abbreviated as "ADSC–LAMS-adipocyte"; (3) 2×10^6 GFP–ADSCs and Rg1 encapsulated in 1 mL of the laminin–alginate microspheres combined with a shredded adipose tissue and abbreviated as "ADSC–G-LAMS–adipocyte". These were injected subcutaneously into the dorsum of the rats.

After 4 weeks, the grafted tissues were harvested, fixed, embedded, sectioned at a thickness of 5 μm, and placed on glass slides. The sections were stained with H&E and immunofluorescence staining for CD31. The sections were observed under an optical microscope and a confocal microscope. In addition, blood element analysis and serological analysis were performed, which included red blood cells (RBC), hemoglobin (HGB), hematocrit (HCT), mean corpuscular volume (MCV), mean corpuscular hemoglobin (MCH), mean corpuscular hemoglobin concentration (MCHC), white blood cells (WBC), neutrophil (NEUT), lymphocyte (LYMPH), monocyte (MONO), eosinophil (EO), and basophil (BASO), alanine aminotransferase (ALT), aspartate aminotransferase (AST), blood urea nitrogen (BUN), and creatinine (CRE).

2.16. Statistics

The results are presented as the mean and standard deviation of at least three independent measurements. One-way analysis of variance (ANOVA) with Tukey's multiple comparisons test was conducted for all the statistical evaluations except, for the one-sided Fisher's exact test for chromosome aberration assay. Differences were considered significant at a p-value of less than 0.05. ($p < 0.05$, *; $p < 0.01$, **; $p < 0.001$, ***).

3. Results

3.1. Functional groups of laminin-modified alginate

The functional groups of the synthesized laminin-modified alginate were analyzed by FTIR spectrophotometry. The infrared spectra were recorded in the wavelength range from 600 cm^{-1}–4000 cm^{-1} (Fig. 1). The FTIR pattern of laminin-modified alginate prepared by a relatively low concentration of sodium periodate and with a long reaction time was similar to the pattern synthesized by the previous method. The absorption bands at 1600 cm^{-1} and 1414 cm^{-1} were corresponding to the asymmetric and symmetric stretching vibrations of the carboxyl group, respectively, and were shown in both alginate and the laminin-modified alginate. The absorption band at 1735 cm^{-1} in the spectrum of the oxidized alginate was corresponding to the aldehyde group (C═O) which was not shown in the alginate and the laminin-modified alginate laminin-alginate. The data confirmed the successful oxidation of the alginate. The aldehyde group in the oxidized alginate could react with the laminin and left no free aldehyde group in the laminin-modified alginate. Moreover, the absorption band at 1470 cm^{-1} in the spectrum of the laminin-modified alginate was attributed to the amide bond (N–H) which was not shown in other groups. The bands at 2850 cm^{-1} and 2920 cm^{-1} were assigned to the asymmetric and symmetric C–H vibrations, respectively. The Schiff bases between 1631.5 cm^{-1} and 1640.9 cm^{-1} attributed to the C═N stretch characteristic of the imino group were not very remarkable, owing to the strong absorption of the carboxyl group and the low concentration of laminin [34].

3.2. Size measurement and SEM examination of developed ADSC–G-LAMS microspheres

The ADSC–G-LAMS microspheres were prepared by bio-electrospraying with a power syringe, as shown in Fig. 2. The

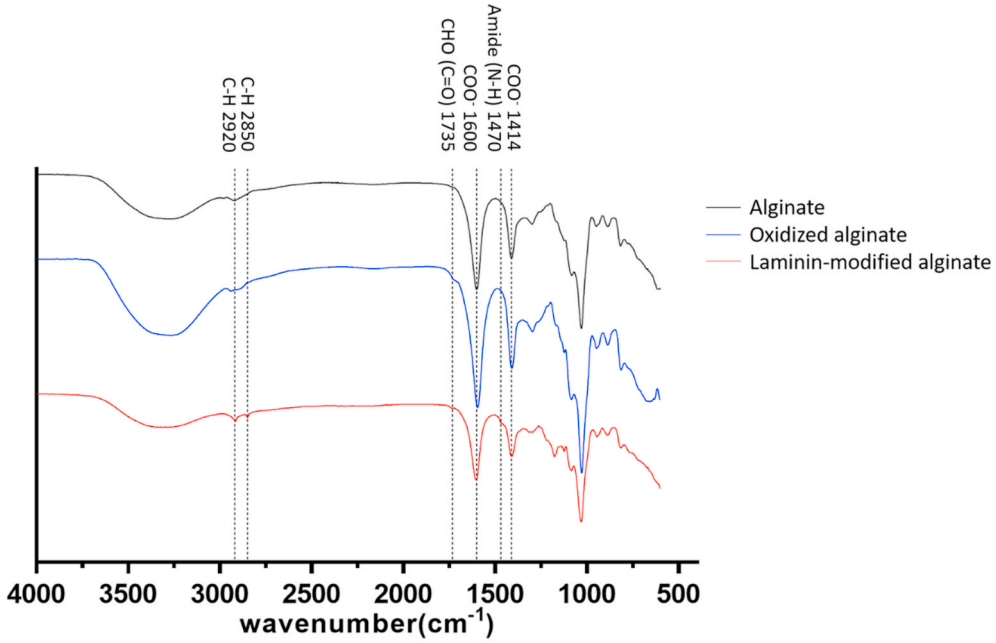

Fig. 1. FTIR spectra of alginate, oxidized alginate, and laminin-modified alginate. Absorption band at 1735 cm^{-1} confirmed formation of aldehyde group (C═O). Absorption band at 1470 cm^{-1} in spectrum of laminin-modified alginate was attributed to amide bond (N–H). Bands at 2850 cm^{-1} and 2920 cm^{-1} were assigned to asymmetric and symmetric C–H vibrations, respectively.

microspheres were uniform with a diameter of 175 ± 27 μm on average at day 0, as shown in Fig. 2(a). The sizes of the spheres were expanded to a mean value of 232 ± 42 μm on days 2, 5, and 9, as shown in Fig. 2(b)–(d), respectively, owing to swelling. The ADSCs appeared as small white spots, indicated as arrows, in the images; they were homogeneously encapsulated in the microspheres. The microspheres were further examined under SEM, where the ADSCs were fully embedded in the G-LAMS microspheres, as shown in Fig. 2(e) and (f).

3.3. Cytotoxicity of G-LAMS microspheres

The cytotoxicity of the G-LAMS microspheres was evaluated using a WST-1 assay, and the cell viability was in terms of the cytotoxicity based on the guidance of ISO-10993 with 3T3-L1 as the target cells. The results showed that the synthesized G-LAMS microspheres were not toxic to the target cells as shown in Fig. 3.

The survival rate of the ADSCs enclosed in the G-LAMS microspheres was examined by a live/dead staining assay (Fig. 4). The living cells were stained with calcein AM, whereas the dead cells were stained with ethidium homodimer-1, which would turn into green and red, respectively, when observed under a fluorescence microscope. As displaced in Fig. 4, more than 99% of the ADSCs were alive in the microspheres at day 1 and day 5. The cell number at day 5 was much greater than that at day 1. We found that the developed G-LAMS microspheres were not toxic to the encapsulated ADSCs and created a good microenvironment for the ADSC proliferation.

3.4. Releasing profiles of Rg1 from G-LAMS microspheres

The cumulative Rg1 released from the laminin-alginate microspheres is presented in Fig. 5. The Rg1 release profile can be seen in two steps. The release rate at the first stage was 270 μg/day, which was owing to the physical desorption of Rg1 on the surface of the microspheres, the so-called initial burst. On the first day, approximately 67.4% was released. The second stage was the relatively slow release of Rg1 at a rate of 12 μg/day, based on the diffusion process. Supposedly, Rg1 was fully released within 5 days.

3.5. Tube formation ability of synthesized G-LAMS microspheres

The tube formation ability of the developed G-LAMS microspheres was determined using Matrigel™ and HUVECs. The experiment was divided into three groups: (1) control group: medium with 2% FBS (Fig. 6(a)); (2) positive control: medium with 2% FBS and ECGS (Fig. 6 (b)); and (3) G-LAMS group: medium with 2% FBS and released Rg1 from G-LAMS microspheres without ECGS (Fig. 6(c)). The results are summarized in Fig. 6(d), based on which the total tube lengths of the positive control and G-LAMS groups increased by 16.1% and 35.9%, respectively, compared to those of the control group. We believe that the Rg1 released from G-LAMS microspheres could maintain the biological activity to induce HUVEC vascularization in the Matrigel™ model.

3.6. Effect of G-LAMS microspheres on HUVEC gene expression

To explore the effect of the G-LAMS microspheres on the HUVEC angiogenesis property, several genes, such as PIK3CA (phosphatidylinositol 3′-kinase (PI3K) catalytic subunit p110α), PIK3R1 (PI3K regulatory subunit p85α), AKT3 (serine/threonine-protein kinase), eNOs (endothelial nitric oxide synthase), were measured by Q-PCR analysis. The results showed that the coculture of the G-LAMS microspheres with HUVECs could affect the upstream genes, PIK3CA, PIK3R1, and AKT3, as shown in Fig. 7(a)–(c), respectively. The gene expression levels were upregulated by 1.35–1.44-fold compared to those of the 2% FBS control group. Concurrently, there was no significant difference in the gene expressions of the LAMS and 2% FBS control groups. However, the eNOs expression (Fig. 7(d)) in the LAMS group was slightly higher than that of the control group. The eNOs expression in the G-LAMS group was 1.75-fold higher than that of the control group. The results indicated that the vascularization of the G-LAMS microspheres to HUVECs proceeded through the pathway of PI3K, Akt, and eNOS from upstream to downstream gene expression.

3.7. Evaluation of G-LAMS microspheres on genotoxicity chromosome aberration assay

CHO cells were used to evaluate the genotoxicity of the G-LAMS

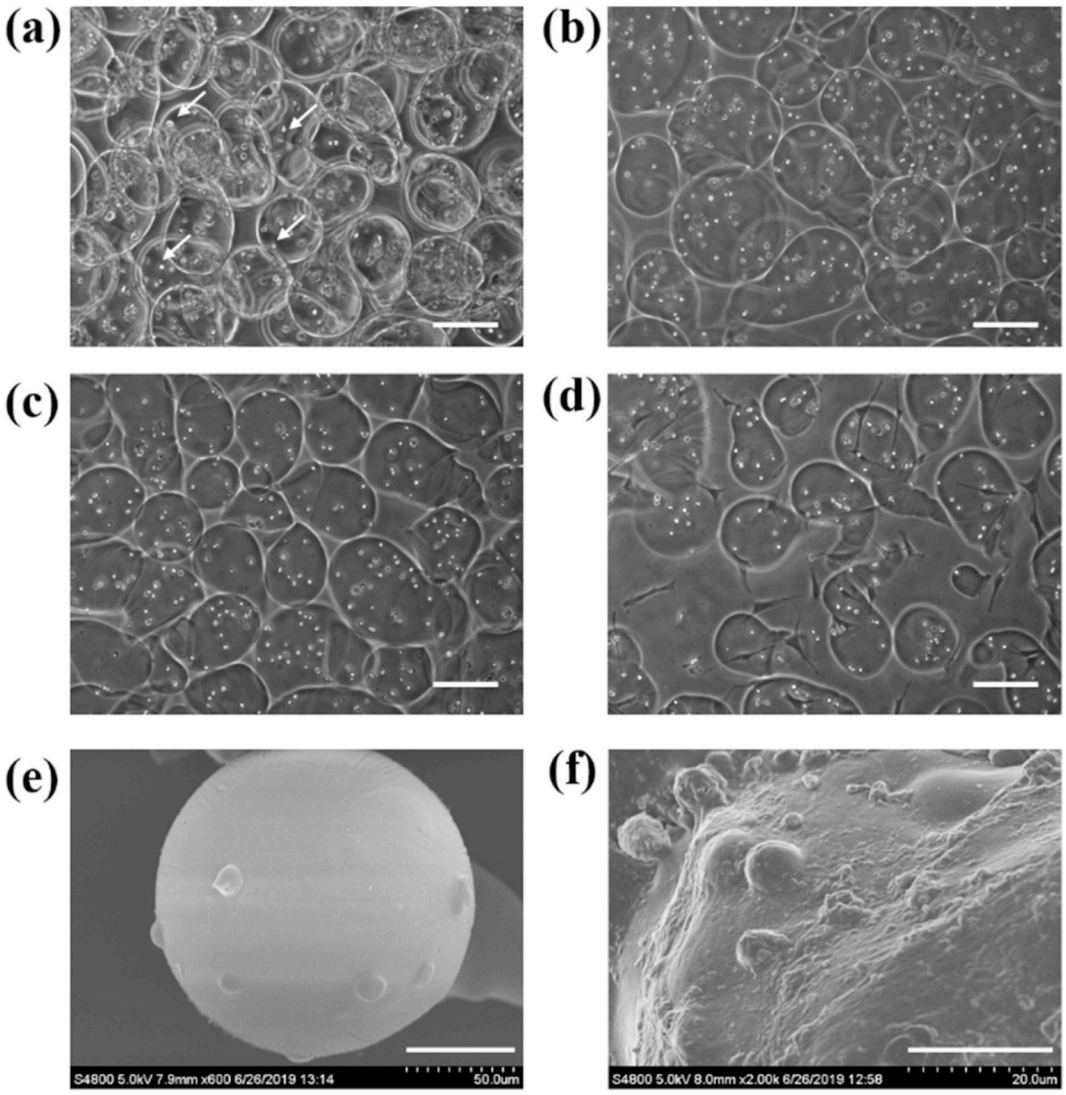

Fig. 2. Morphology and microstructure of laminin-alginate microspheres were observed by optical microscopy and SEM. Images were captured using an optical microscope at (a) Day 0, (b) Day 2, (c) Day 5, and (d) Day 9 after ADSC–G-LAMS preparation. Arrows indicate ADSCs encapsulated in G-LAMS microspheres. Scale bar = 200 μm. SEM images were captured on Day 5 at (e) 600 × magnification, scale bar = 50 μm and (f) 2000 × magnification, scale bar = 20 μm.

microspheres, where the control group was the blank medium and the experimental group was an extract of the G-LAMS microspheres (Fig. 8). A total of 70 well-spread chromosomes could be examined under a differential interference contrast microscope using the Giemsa stain. Fisher's exact test was conducted to analyze the statistical data. There was no significant difference in the chromosome aberrations of the control and experimental groups, as summarized in Table 1.

3.8. Histological and immunofluorescence analysis

The adipogenesis of the developed G-LAMS encapsulated ADSCs with adipocytes (ADSC–G-LAMS–adipocyte) was evaluated by CD31 immunostaining and H&E staining in the fourth week of subcutaneous injection. The nuclei were stained with 4′,6-diamidino-2-phenylindole (DAPI) and GFP-positive cells corresponded to the ADSCs, which appeared blue and green under a confocal microscope (Fig. 9(a)). CD31, the major marker of endothelial cells, was in red. Quantification of the angiogenesis was achieved by calculating the relative cell number in the CD31 fluorescence image using the ImageJ software (Fig. 9(b)). The endothelial cell numbers in the ADSC–LAMS–adipocyte and ADSC–G-LAMS–adipocyte groups were much higher than those in the ADSC–adipocyte group. In contrast to the microspheres without Rg1 (ADSC–LAMS–adipocyte), the microspheres containing Rg1 (ADSC–G-LAMS–adipocyte) showed the highest number of endothelial cells in adipose tissues (Fig. 9).

The H&E stain also presented results similar to those of CD31. The neo-blood vessels, indicated by arrows in Fig. 9(a) in the ADSC–G-LAMS–adipocyte group, were much larger than those of the other two groups. The injected microspheres (asterisk) were fully integrated into the host tissue.

3.9. Blood element analysis and serological analysis

Whole blood was collected from the rats, before sacrifice, for blood element analysis and serological analysis. Compared to the reference value (Charles River Laboratories, CD® IGS Rat Model Information Sheet), the data of the blood element analysis (Table 2) and serological analysis (Table 3) were all within the normal range. The results indicated that the laminin-alginate microspheres with or without Rg1 showed no systemic toxicity.

4. Discussion

Alginate is a biodegradable polymer in which cells can be

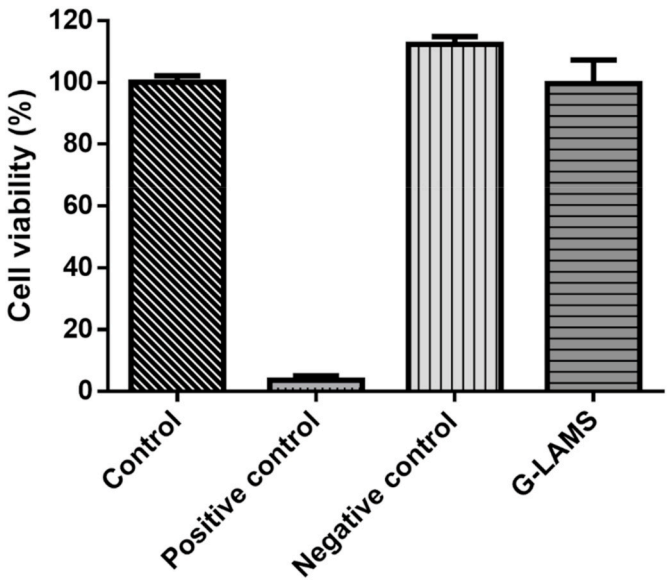

Fig. 3. Cell viability of G-LAMS microspheres was evaluated by 3T3-L1 viability according to guidance of ISO-10993; results were terms of cytotoxicity. 3T3-L1 cultured in DMEM was set as the control group. ZDEC extract was selected as the positive control group, Al_2O_3 extract as the negative control group.

encapsulated and transplanted into the animals for numerous applications [35,36]. However, alginate lacks domains for cell recognition. Laminin, a major extracellular matrix glycoprotein, has been reported to play an important role in influencing cell differentiation, migration, and adhesion in the early embryonic stage [22–24,37].

In polymer modification, sodium periodate is often used as the oxidizing agent in synthesizing oxidized polymer [38–40]. In this study, laminin was modified by alginate by a relatively low concentration of $NaIO_4$ with a long reaction time to synthesize achieve better cell viability and lower cytotoxicity, as shown in Figs. 1–4. The developed laminin-modified alginate was mixed with ADSCs and Rg1 in a medium; thereafter, it was sprayed into a $CaCl_2$ solution by bio-electrospraying with a power syringe to form ADSC–G-LAMS microspheres. The prepared ADSC–G-LAMS microspheres were collected and combined with adipocytes to produce the necessary growth factors to make ADSCs towards the adipogenic pathway.

It has been reported that the diameter of the microspheres should be smaller than 350 μm to minimize the fibrosis reaction [41]. The fibrosis reaction can cause fibrous capsule contraction and results in an implanted breast with low tactile quality [42]. The average diameter of the microspheres prepared using the bio-electrospray method was 232 ± 42 μm (Fig. 2), which was convenient for injection. In addition, the small diameter could shorten the diffusion distance of the nutrition and oxygen, to make encapsulated cells with high proliferation and survival rates (Figs. 3 and 4).

Ginsenoside Rg1 is a bioactive extract from Panax ginseng, which has commonly used as the Chinese herbal medicine [43]. It has estrogen-like properties; therefore, it can interact with a glucocorticoid receptor and activate nitric oxide synthase [44,45]. Nitric oxide is well known to be an important factor in the mediation of angiogenesis and the proliferation of endothelial cells [44,46]. It was noted that the bioactivity of Rg1 was not affected by the temperature, pH, and solvents, compared with protein-based growth factors [47]. Rg1 also affects mesenchymal stem cells (MSCs) proliferation, differentiation, and apoptosis [48]. One study showed that Rg1 could promote endothelial differentiation of human MSCs *in vitro* [49]. Other results also showed that Rg1 could attract the rabbit bone marrow MSCs to migrate to local myocardial tissues and differentiate into vascular endothelial cells for the capillary regeneration of infarcted myocardium tissue *in vivo* [50]. In addition, it was reported that Rg1 mixed with collagen and increased the micro-vessel density in the nude mice model for soft tissue regeneration [51]. In this study, Rg1 was selected as a bioactive molecule, enclosed in the laminin-modified alginate microspheres, and proved the tube formation ability using the Matrigel™ model (Figs. 5 and 6). In the study of the Rg1 release profile, an initial burst occurred on the first day. We believe that it is necessary to provide sufficient signals to attract the MSCs for tissue reconstruction (Fig. 9). The sustained release of Rg1 was to induce encapsulated ADSCs or homing MSCs towards neo-vascularization to sustain the injected ADSCs or adipocytes survival, to combine tissue growth and repair.

In this study, several genes were selected to confirm that PI3K/AKT/

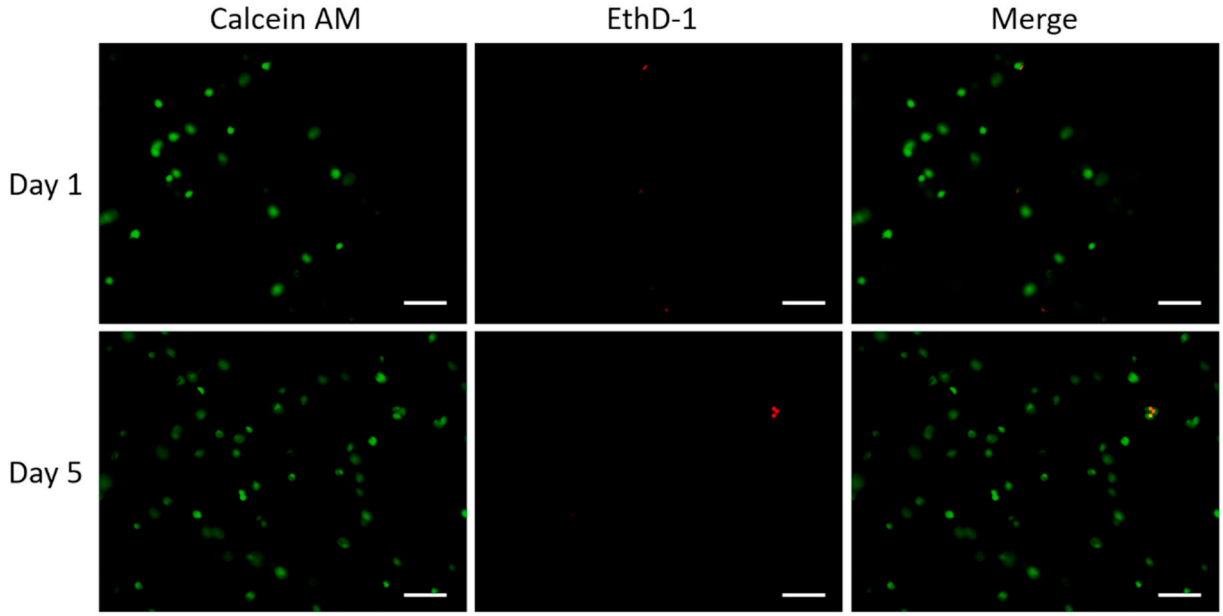

Fig. 4. Evaluation of ADSCs in ADSC–G-LAMS by a live/dead staining assay. ADSCs were encapsulated in G-LAMS microspheres and analyzed at day 1 and day 5. The living cells in green were stained with calcein AM, and the dead cells colored in red were stained with ethidium homodimer-1 (EthD-1). Scale bar = 100 μm. (For interpretation of the references to color in this figure legend, the reader is referred to the Web version of this article.)

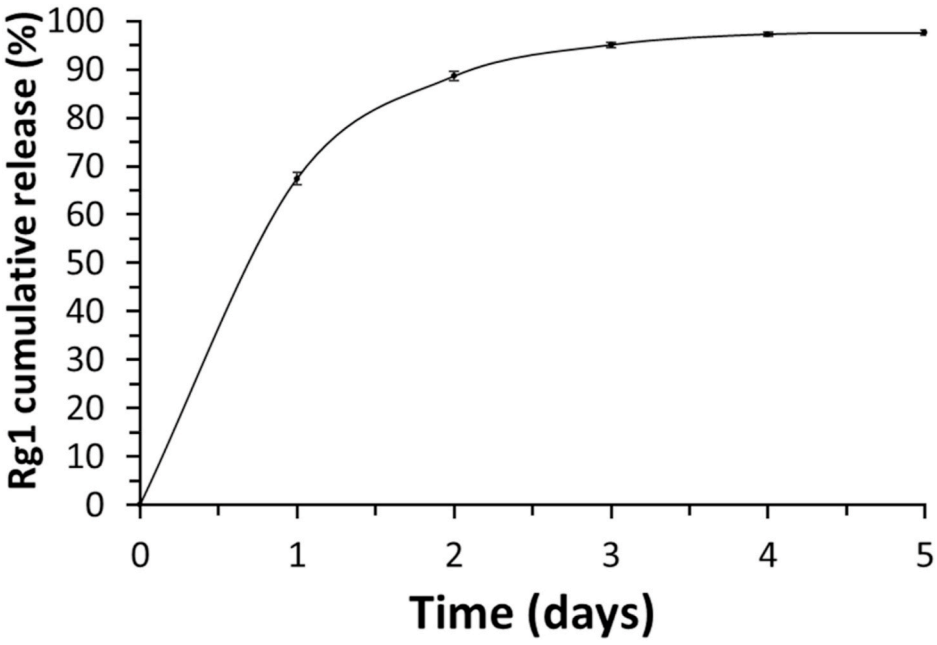

Fig. 5. Releasing profiles of Rg1 from G-LAMS microspheres. Cumulative Rg1 released curve was measured by HPLC.

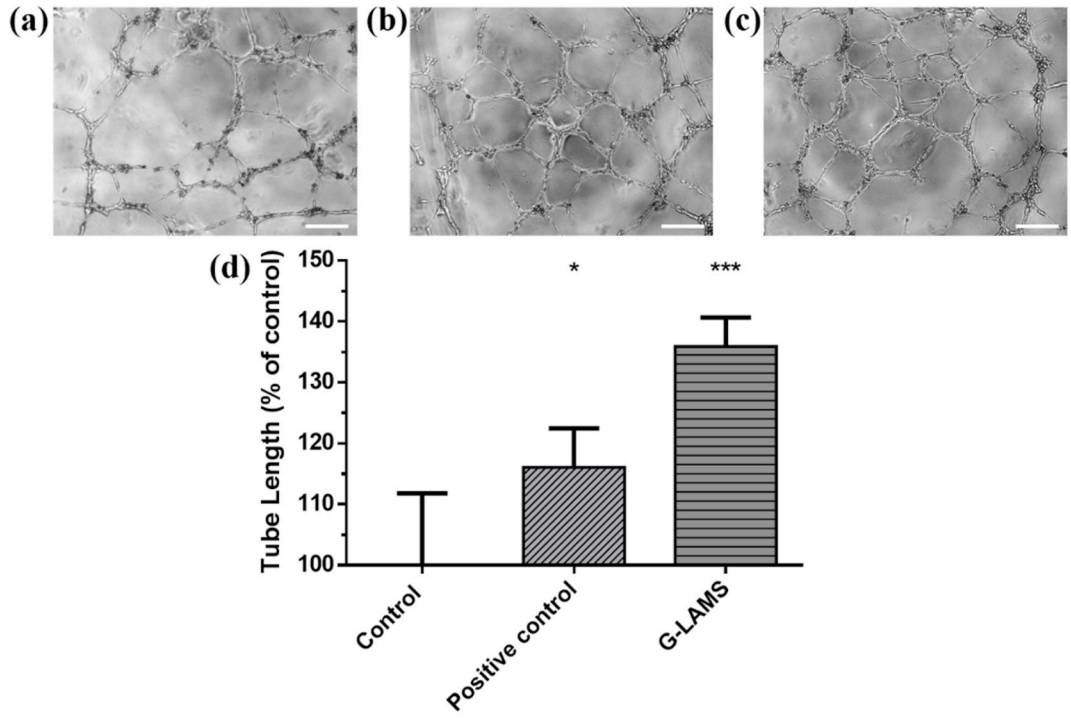

Fig. 6. Tube formation ability of Rg1 released from G-LAMS microspheres was tested by HUVEC tube formation assay with Matrigel™, where (a) Control: medium with 2% FBS (b) Positive control: medium with 2% FBS and endothelial cell growth supplement (ECGS); and (c) G-LAMS: medium with 2% FBS and released Rg1 from G-LAMS microspheres without ECGS. Scale bar = 200 μm. (d) Quantification using ImageJ software. ($p < 0.05$, *; $p < 0.001$, ***, compared to control group by one-way ANOVA with Tukey's multiple comparisons test.)

eNOs was the major pathway to induce HUVEC vascularization under Rg1 stimulation (Fig. 7(a)–7(d)). In addition, we noticed that the eNOs gene expression in the LAMS microspheres was much higher than that in the control group; however, there were no significant differences in the gene expression related to the PI3K/AKT pathway. It has been shown that laminin can influence endothelial shear sensing and mechanotransduction through focal adhesion kinase (FAK). Shear-induced eNOs synthesis may occur in endothelial cells [52–54]. We believe that the difference in the eNOs expressions of the LAMS and control group might be partially attributed to laminin, instead of Rg1. The detailed mechanism of the laminin action is not discussed in detail in this paper; however, it still yields a promising result that the combination of Rg1 with laminin-modified alginate carriers can have significant effects on angiogenic properties. The results of the chromosome aberration by the CHO cells and Giemsa stain showed that the synthesized G-LAMS microspheres were not associated with genotoxicity, as shown

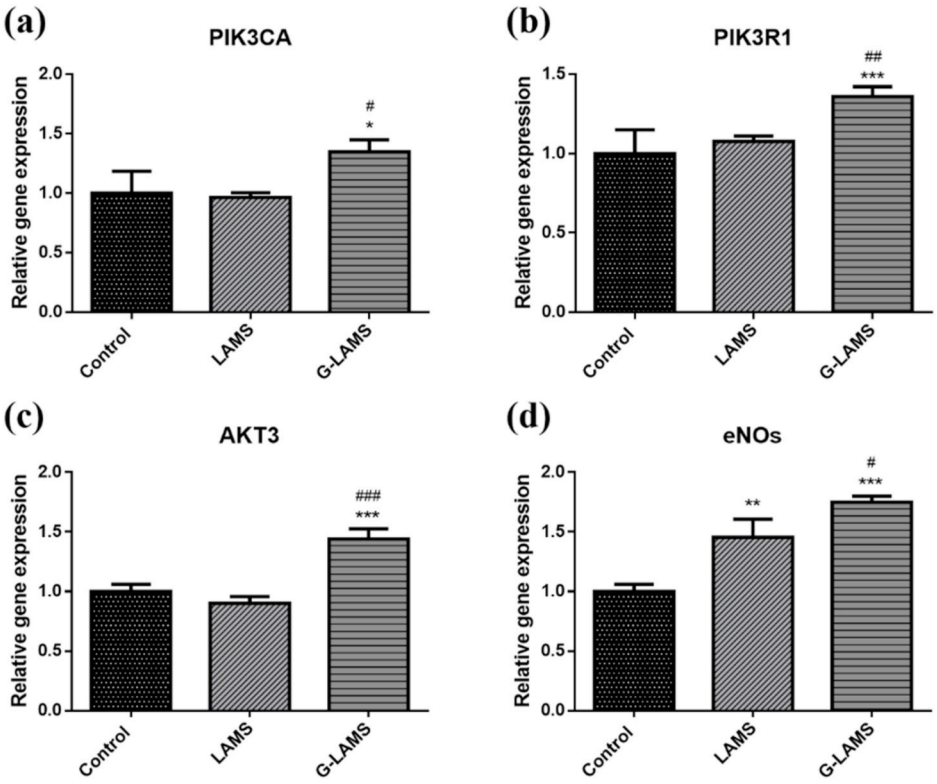

Fig. 7. Gene expression of HUVECs after starvation for 4 h and treatment with materials for 1 h. Relative (a) PIK3CA, (b) PIK3R1, (c) AKT3, and (d) eNOs gene expressions were measured by Q-PCR and normalized by GAPDH gene expression. ($p < 0.05$, *; $p < 0.01$, **; $p < 0.001$, *** compared to control group; $p < 0.05$, #; $p < 0.01$, ##; $p < 0.001$, ### compared to LAMS group by one-way ANOVA with Tukey's multiple comparisons test.)

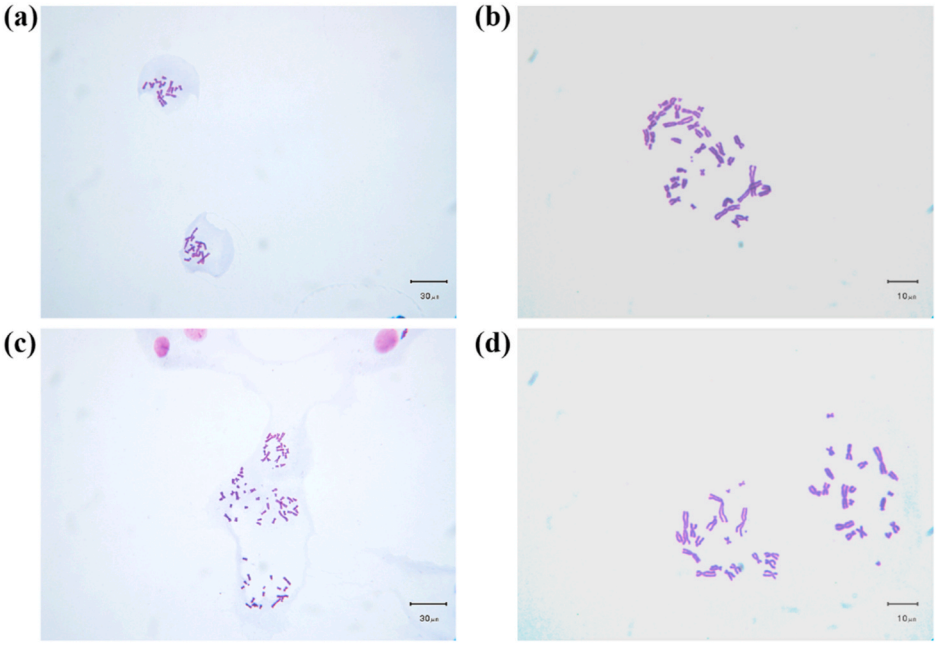

Fig. 8. Genotoxicity assay evaluation using CHO cell chromosome aberration assay. CHO cells were treated with (a) negative control observed under 40 × magnification and (b) negative control examined under 100 × magnification; aberrations were compared with (c) experimental group with G-LAMS extract observed under 40 × magnification and (d) experimental group added with G-LAMS extract observed under 100 × magnification.

in Fig. 8 and summarized in Table 1.

In adipose tissue engineering, new blood vessel formation is important for the transplanted cell survival and reducing the grafting volume shrinkage [55]. In animal studies, the materials were cocultured with autologous adipose tissue, forming an injectable engineered fat. Adipocytes have been reported to release various signals to regulate local MSCs or ADSCs towards adipogenic differentiation [56–59]. The results of the animal study showed that the ADSC–G-LAMS–adipocyte group

Table 1
Chromosome aberrations of the negative control and G-LAMS treated CHO cells.[a].

Treatment	Aberrant metaphases	Total metaphases	Aberration frequency	P-value
Control	5	70	0.071	
G-LAMS	2	70	0.029	NS

[a] Summary data of genotoxicity results from negative control group and G-LAMS treated CHO cells. P-value derived from Fisher's exact test. NS = Not significant.

exhibited the highest number of neo-blood vessels and endothelial cells with remarkable adipogenesis, as displaced in Fig. 9. The results of the blood element analysis and serological analysis further confirmed the safety of the prepared cell-laden adipo-graft (Tables 2 and 3).

In this study, the efficacy of the developed ADSC–G-LAMS microspheres was determined by comparing them with ADSC–LAMS microspheres and ADSCs. The Rg1 release from the ADSC–G-LAMS microspheres enhanced the angiogenesis. ADSCs and adipocytes played important roles in the adipogenesis. These results were confirmed both *in vitro* and *in vivo*. In the future, the microspheres prepared in this study might be developed to deliver other bioactive molecules, growth factors, and drugs for other applications in stem cell therapy and tissue engineering.

5. Conclusion

In this study, we successfully synthesized laminin-modified alginate to mimic the embryonic environment. The bioactive ADSC–G-LAMS microspheres prepared by the bio-electrospray method and provided a good environment to allow the ADSCs to survive, proliferate, and shift towards the desired differentiation pathway without cytotoxicity, genotoxicity, and systemic toxicity. The sustained release of Rg1 could induce the encapsulated ADSCs or homing MSCs towards neovascularization to enhance the ADSC or adipocyte survival rate to join

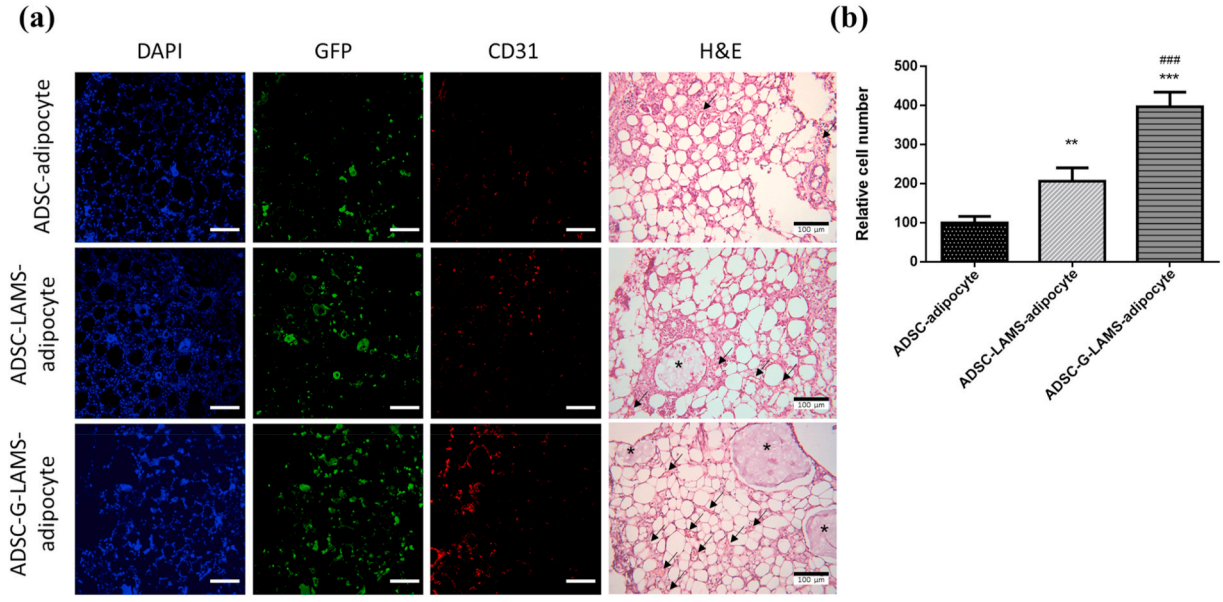

Fig. 9. *In vivo* analysis of grafts after 4 weeks (a) Immunofluorescence staining of CD31 on adipose tissue sections from implant site. CD31 was used as endothelial cell marker. Nuclei were stained with DAPI, and GFP-positive cells were observed by confocal microscopy. In H&E staining, arrows indicate blood vessels, and asterisks indicate the implanted microspheres. Scale bar = 100 μm, (b) Quantification of angiogenesis was determined by calculating relative cell number in CD31 fluorescence image by ImageJ. (Data in (b) were measured by four independent experiments, and at least five fields were taken per section.) ($p < 0.05$, *; $p < 0.01$, **; $p < 0.001$, ***, compared to the ADSC–adipocyte group; $p < 0.05$, #; $p < 0.01$, ##; $p < 0.001$, ### compared to the ADSC–LAMS–adipocyte group by one-way ANOVA with Tukey's multiple comparisons test.).

Table 2
Blood element analysis.

	ADSC–adipocyte	ADSC–LAMS–adipocyte	ADSC–G-LAMS–adipocyte	Reference[a)]
RBC (M/μL)	8.27 ± 0.41	7.67 ± 0.36	8.03 ± 0.42	7.37 ± 1.09
HGB (g/dL)	16.90 ± 0.62	15.20 ± 0.89	15.57 ± 1.03	16.52 ± 2.72
HCT (%)	52.57 ± 3.33	44.12 ± 4.20	47.17 ± 2.84	48.45 ± 7.14
MCV (fL)	63.57 ± 1.60	60.16 ± 1.23	58.77 ± 0.83	65.49 ± 6.46
MCH (pg)	20.47 ± 0.80	19.80 ± 0.35	19.37 ± 0.34	22.40 ± 1.35
MCHC (g/dL)	32.20 ± 1.04	32.94 ± 0.26	33.00 ± 0.22	34.10 ± 2.34
PLT (K/μL)	1274.67 ± 339.01	1109.80 ± 170.04	1182.67 ± 21.14	1583.22 ± 378.23
WBC (K/μL)	9.09 ± 0.62	9.10 ± 2.59	9.03 ± 1.90	10.17 ± 3.72
NEUT (K/μL)	2.72 ± 0.85	2.43 ± 1.75	3.25 ± 2.03	2.62 ± 1.24
LYMPH (K/μL)	5.49 ± 1.10	6.24 ± 2.35	5.18 ± 0.23	6.73 ± 2.64
MONO (K/μL)	0.72 ± 0.43	0.25 ± 0.07	0.41 ± 0.10	0.62 ± 0.28
EO (K/μL)	0.14 ± 0.05	0.16 ± 0.04	0.16 ± 0.05	0.15 ± 0.16
BASO (K/μL)	0.02 ± 0.01	0.02 ± 0.02	0.04 ± 0.01	0.04 ± 0.05

[a)] Charles River Laboratories, CD® IGS Rat Model Information Sheet. RBC: red blood cell; HGB: hemoglobin; HCT: hematocrit; MCV: mean corpuscular volume: MCH: mean corpuscular hemoglobin; MCHC: mean corpuscular hemoglobin concentration; PLT: platelet; WBC: white blood cell; NEUT: neutrophil; LYMPTH: lymphocyte; MONO: monocyte; EO: eosinophil; BASO: basophil.

Table 3
Serological analysis.

	ADSC–adipocyte	ADSC–LAMS–adipocyte	ADSC–G-LAMS–adipocyte	Reference[a)]
ALT (U/L)	46.25 ± 5.54	40.80 ± 2.56	48.25 ± 13.37	56.72 ± 32.40
AST (U/L)	82.40 ± 6.06	82.12 ± 6.64	114.45 ± 54.42	111.88 ± 65.11
BUN (mg/dL)	17.92 ± 2.84	16.25 ± 1.71	16.73 ± 1.93	13.45 ± 4.19
Crea (mg/dL)	0.45 ± 0.11	0.50 ± 0.15	0.43 ± 0.04	0.47 ± 0.10

[a)] Charles River Laboratories, CD® IGS Rat Model Information Sheet. ALT: alanine aminotransferase; AST: aspartate aminotransferase; BUN: blood urea nitrogen; Crea: creatinine.

tissue growth and repair with adipogenesis for breast reconstruction after lumpectomy. These findings fully support that the ADSC–G-LAMS microspheres can be potential scaffolds for stem cells and angiogenic factor carriers for adipose tissue engineering.

Declaration of competing interest

The authors declare no conflict of interest.

CRediT authorship contribution statement

I-Hsuan Yang: Methodology, Validation, Formal analysis, Writing - original draft. **Yo-Shen Chen:** Methodology, Writing - review & editing, Supervision. **Jia-Jing Li:** Methodology. **Ya-Jyun Liang:** Methodology. **Tzu-Chieh Lin:** Methodology. **Subhaini Jakfar:** Methodology. **Minal Thacker:** Methodology. **Shinn-Chih Wu:** Resources. **Feng-Huei Lin:** Conceptualization, Methodology, Formal analysis, Writing - review & editing, Supervision.

Acknowledgements

This study was supported by the National Health Research Institutes (BN-109-PP-01), National Health Research Institutes and Central Government S & T grant, Taiwan (109-1901-01-19-07), and subsidized by Ministry of Science and Technology and National Taiwan University (NTU), Taiwan.

Appendix A. Supplementary data

Supplementary data related to this article can be found at https://doi.org/10.1016/j.bioactmat.2020.11.029.

References

[1] R.L. Siegel, K.D. Miller, A. Jemal, Cancer statistics, Ca - Cancer J. Clin. 69 (1) (2019) 7–34.
[2] A.C. Society, Breast cancer facts & figures 2019–2020, Am. Cancer Soc (2019) 1–44.
[3] K.J. Burg, B. Inskeep, T.C. Burg, Breast Tissue Engineering: Reconstruction Implants and Three-Dimensional Tissue Test Systems, Principles of Tissue Engineering, Elsevier, 2014, pp. 727–749.
[4] E.J. Giltay, H.B. Moens, A.H. Riley, R.G. Tan, Silicone breast prostheses and rheumatic symptoms: a retrospective follow up study, Ann. Rheum. Dis. 53 (3) (1994) 194–196.
[5] R. Gayou, R. Rudolph, Capsular contraction around silicone mammary prostheses, Ann. Plast. Surg. 2 (1) (1979) 62–71.
[6] H. Holmström, The free abdominoplasty flap and its use in breast reconstruction: an experimental study and clinical case report, Scand. J. Plast. Reconstr. Surg. 13 (3) (1979) 423–427.
[7] J.C. Selber, J.E. Kurichi, S.J. Vega, S.S. Sonnad, J.M. Serletti, Risk factors and complications in free TRAM flap breast reconstruction, Ann. Plast. Surg. 56 (5) (2006) 492–497.
[8] P.S. Gill, J.P. Hunt, A.B. Guerra, F.J. Dellacroce, S.K. Sullivan, J. Boraski, S. E. Metzinger, C.L. Dupin, R.J. Allen, A 10-year retrospective review of 758 DIEP flaps for breast reconstruction, Plast. Reconstr. Surg. 113 (4) (2004) 1153–1160.
[9] R.D. Rehnke, I. M Asher Schusterman, J.M. Clarke, B.C. Price, U. Waheed, R. E. Debski, S.F. Badylak, J.P. Rubin, Breast reconstruction using a three-dimensional absorbable mesh scaffold and autologous fat grafting: a composite strategy based on tissue-engineering principles, Plast. Reconstr. Surg. 146 (4) (2020) 409e–413e.
[10] I. Van Nieuwenhove, L. Tytgat, M. Ryx, P. Blondeel, F. Stillaert, H. Thienpont, H. Ottevaere, P. Dubruel, S. Van Vlierberghe, Soft tissue fillers for adipose tissue regeneration: from hydrogel development toward clinical applications, Acta Biomater. 63 (2017) 37–49.
[11] J.P. Vacanti, A. Atala, D.J. Mooney, R.S. Langer, Breast Tissue Engineering, Google Patents, 1998.
[12] J.M. Gimble, A.J. Katz, B.A. Bunnell, Adipose-derived stem cells for regenerative medicine, Circ. Res. 100 (9) (2007) 1249–1260.
[13] Y. Xu, C. Chen, P.B. Hellwarth, X. Bao, Biomaterials for stem cell engineering and biomanufacturing, Bioactive materials 4 (2019) 366–379.
[14] Y. Luo, G. Engelmayr, D.T. Auguste, L. da Silva Ferreira, J.M. Karp, R. Saigal, R. Langer, 3D Scaffolds, Principles of Tissue Engineering, Elsevier, 2014, pp. 475–494.
[15] A. Jaklenec, E. Wan, M.E. Murray, E. Mathiowitz, Novel scaffolds fabricated from protein-loaded microspheres for tissue engineering, Biomaterials 29 (2) (2008) 185–192.
[16] I. Van Nieuwenhove, L. Tytgat, M. Ryx, P. Blondeel, F. Stillaert, H. Thienpont, H. Ottevaere, P. Dubruel, S.J.A.b. Van Vlierberghe, Soft tissue fillers for adipose tissue regeneration: from hydrogel development toward clinical applications 63 (2017) 37–49.
[17] Y. Kimura, M. Ozeki, T. Inamoto, Y. Tabata, Adipose tissue engineering based on human preadipocytes combined with gelatin microspheres containing basic fibroblast growth factor, Biomaterials 24 (14) (2003) 2513–2521.
[18] C. Halberstadt, C. Austin, J. Rowley, C. Culberson, A. Loebsack, S. Wyatt, S. Coleman, L. Blacksten, K. Burg, D.J.T.e. Mooney, A hydrogel material for plastic and reconstructive applications injected into the subcutaneous space of a sheep 8 (2) (2002) 309–319.
[19] K.Y. Lee, D.J. Mooney, Alginate: properties and biomedical applications, Prog. Polym. Sci. 37 (1) (2012) 106–126.
[20] Y.-S. Chen, Y.-S. Hsueh, Y.-Y. Chen, C.-Y. Lo, H.-C. Tai, F.-H. Lin, Evaluation of a laminin-alginate biomaterial, adipocytes, and adipocyte-derived stem cells interaction in animal autologous fat grafting model using 7-Tesla magnetic resonance imaging, J. Mater. Sci. Mater. Med. 28 (1) (2017) 18.
[21] J.H. Hwang, O.Y. Kim, A.R. Kim, J.Y. Bae, S.M. Jeong, J.B. Shim, K.H. Yoon, D. Lee, G. Khang, Effect of purified alginate microcapsules on the regeneration of chondrocytes, Biomed. Eng.: Applications, Basis and Communications 24 (3) (2012) 185–195.
[22] I. Leivo, A. Vaheri, R. Timpl, J. Wartiovaara, Appearance and distribution of collagens and laminin in the early mouse embryo, Dev. Biol. 76 (1) (1980) 100–114.
[23] E. Hohenester, P.D. Yurchenco, Laminins in basement membrane assembly, Cell Adhes. Migrat. 7 (1) (2013) 56–63.
[24] S. Li, D. Edgar, R. Fässler, W. Wadsworth, P.D. Yurchenco, The role of laminin in embryonic cell polarization and tissue organization, Dev. Cell 4 (5) (2003) 613–624.
[25] Y.-S. Hsueh, Y.-S. Chen, H.-C. Tai, O. Mestak, S.-C. Chao, Y.-Y. Chen, Y. Shih, J.-F. Lin, M.-J. Shieh, F.-H. Lin, Laminin-alginate beads as preadipocyte carriers to enhance adipogenesis in vitro and in vivo, Tissue Eng. 23 (5–6) (2017) 185–194.
[26] M. Lovett, K. Lee, A. Edwards, D.L. Kaplan, Vascularization strategies for tissue engineering, Tissue Eng. B Rev. 15 (3) (2009) 353–370.
[27] C.D. Ley, M.W. Olsen, E.L. Lund, P.E. Kristjansen, Angiogenic synergy of bFGF and VEGF is antagonized by Angiopoietin-2 in a modified in vivo Matrigel assay, Microvasc. Res. 68 (3) (2004) 161–168.
[28] D.F. Lazarous, M. Scheinowitz, M. Shou, E. Hodge, M.S. Rajanayagam, S. Hunsberger, W.G. Robison Jr., J.A. Stiber, R. Correa, S.E. Epstein, Effects of chronic systemic administration of basic fibroblast growth factor on collateral development in the canine heart, Circulation 91 (1) (1995) 145–153.
[29] J. Karar, A. Maity, PI3K/AKT/mTOR pathway in angiogenesis, Front. Mol. Neurosci. 4 (2011) 51.
[30] K.W. Leung, Y.-K. Cheng, N.K. Mak, K.K. Chan, T. David Fan, R.N. Wong, Signaling pathway of ginsenoside-Rg1 leading to nitric oxide production in endothelial cells, FEBS Lett. 580 (13) (2006) 3211–3216.
[31] K.W. Leung, Y.L. Pon, R.N. Wong, A.S. Wong, Ginsenoside-Rg1 induces vascular endothelial growth factor expression through the glucocorticoid receptor-related phosphatidylinositol 3-kinase/Akt and β-catenin/T-cell factor-dependent pathway in human endothelial cells, J. Biol. Chem. 281 (47) (2006) 36280–36288.
[32] S. Sengupta, S.-A. Toh, L.A. Sellers, J.N. Skepper, P. Koolwijk, H.W. Leung, H.-W. Yeung, R.N. Wong, R. Sasisekharan, T.-P.D. Fan, Modulating angiogenesis: the yin and the yang in ginseng, Circulation 110 (10) (2004) 1219–1225.
[33] B.A. Bunnell, M. Flaat, C. Gagliardi, B. Patel, C. Ripoll, Adipose-derived stem cells: isolation, expansion and differentiation, Methods 45 (2) (2008) 115–120.
[34] L. Marin, D. Ailincai, M. Mares, E. Paslaru, M. Cristea, V. Nica, B.C. Simionescu, Imino-chitosan biopolymeric films. Obtaining, self-assembling, surface and antimicrobial properties, Carbohydr. Polym. 117 (2015) 762–770.

[35] S. Deepthi, R. Jayakumar, Alginate nanobeads interspersed fibrin network as in situ forming hydrogel for soft tissue engineering, Bioactive materials 3 (2) (2018) 194–200.
[36] M. Nie, G. Chen, C. Zhao, J. Gan, M. Alip, Y. Zhao, L. Sun, Bio-inspired adhesive porous particles with human MSCs encapsulation for systemic lupus erythematosus treatment, Bioactive materials 6 (1) (2020) 84–90.
[37] S.D. Silva-Barbosa, G.S. Butler-Browne, W. de Mello, I. Riederer, J.P. Di Santo, W. Savino, V. Mouly, Human myoblast engraftment is improved in laminin-enriched microenvironment, Transplantation 85 (4) (2008) 566–575.
[38] W.-Y. Su, Y.-C. Chen, F.-H. Lin, Injectable oxidized hyaluronic acid/adipic acid dihydrazide hydrogel for nucleus pulposus regeneration, Acta Biomater. 6 (8) (2010) 3044–3055.
[39] M.-Y. Hsiao, P.C. Lin, A.-C. Lin, Y.-W. Wu, W.-S. Chen, F.-H. Lin, Oxidized hyaluronic acid/adipic acid dihydrazide hydrogel as drug-carrier for cytoprotective medications—preliminary results, Biomed. Eng.: Applications, Basis and Communications 31 (5) (2019) 1950036.
[40] C.-Y. Kuan, Y.-Y. Lin, C.-Y. Chen, C.-C. Yang, C.-Y. Chi, C.-H. Li, G.-C. Dong, F.-H. Lin, The preparation of oxidized methylcellulose crosslinked by adipic acid dihydrazide loaded with vitamin C for traumatic brain injury, J. Mater. Chem. B 7 (29) (2019) 4499–4508.
[41] R. Robitaille, J.F. Pariseau, F.A. Leblond, M. Lamoureux, Y. Lepage, J.P. Hallé, Studies on small (< 350 μm) alginate-poly-L-lysine microcapsules. III. Biocompatibility of smaller versus standard microcapsules, J. Biomed. Mater. Res.: An Official Journal of The Society for Biomaterials, The Japanese Society for Biomaterials, and The Australian Society for Biomaterials and the Korean Society for Biomaterials 44 (1) (1999) 116–120.
[42] E. Donnely, M. Griffin, P. Butler, Breast reconstruction with a tissue engineering and regenerative medicine approach (systematic review), Ann. Biomed. Eng. (2019) 1–17.
[43] T. Zhu, Y. Cui, M. Zhang, D. Zhao, G. Liu, J. Ding, Engineered three-dimensional scaffolds for enhanced bone regeneration in osteonecrosis, Bioactive Materials 5 (3) (2020) 584–601.
[44] R.Y. Chan, W.-F. Chen, A. Dong, D. Guo, M.-S. Wong, Estrogen-like activity of ginsenoside Rg1 derived from Panax notoginseng, J. Clin. Endocrinol. Metabol. 87 (8) (2002) 3691–3695.
[45] L.W. Cheung, K.W. Leung, C.K. Wong, R.N. Wong, A.S. Wong, Ginsenoside-Rg1 induces angiogenesis via non-genomic crosstalk of glucocorticoid receptor and fibroblast growth factor receptor-1, Cardiovasc. Res. 89 (2) (2011) 419–425.
[46] J.P. Cooke, D.W. Losordo, Nitric Oxide and Angiogenesis, Am Heart Assoc, 2002.
[47] L.-C. Yu, S.-C. Chen, W.-C. Chang, Y.-C. Huang, K.M. Lin, P.-H. Lai, H.-W. Sung, Stability of angiogenic agents, ginsenoside Rg1 and Re, isolated from Panax ginseng: in vitro and in vivo studies, Int. J. Pharm. 328 (2) (2007) 168–176.
[48] F. He, C. Yu, T. Liu, H. Jia, Ginsenoside Rg1 as an effective regulator of mesenchymal stem cells, Front. Pharmacol. 10 (2020) 1565.
[49] W. He, W.-K. Wu, Y.-L. Wu, X.-H. Yang, Q.-X. Lin, W.-H. Yu, Ginsenoside-Rg1 mediates microenvironment-dependent endothelial differentiation of human mesenchymal stem cells in vitro, J. Asian Nat. Prod. Res. 13 (1) (2011) 1–11.
[50] N. Wang, C. Lu, X. Chen, Study on effect of ginsenoside Rg1 in promoting myocardiac vascular endothelial cell regeneration through induction on bone marrow stem cell's migration and differentiation in rabbits of myocardial infarction, Zhongguo Zhong xi yi jie he za zhi Zhongguo Zhongxiyi jiehe zazhi= Chinese journal of integrated traditional and Western medicine 25 (10) (2005) 916–919.
[51] F.-T. Xu, Z.-J. Liang, H.-M. Li, Q.-L. Peng, M.-H. Huang, D.-Q. Li, Y.-D. Liang, G.-Y. Chi, D.-H. Li, B.-C. Yu, Ginsenoside Rg1 and platelet-rich fibrin enhance human breast adipose-derived stem cells function for soft tissue regeneration, Oncotarget 7 (23) (2016) 35390.
[52] L.F. Yousif, J. Di Russo, L. Sorokin, Laminin isoforms in endothelial and perivascular basement membranes, Cell Adhes. Migrat. 7 (1) (2013) 101–110.
[53] T. Gloe, S. Riedmayr, H.-Y. Sohn, U. Pohl, The 67-kDa laminin-binding protein is involved in shear stress-dependent endothelial nitric-oxide synthase expression, J. Biol. Chem. 274 (23) (1999) 15996–16002.
[54] Y.S. Chatzizisis, A.U. Coskun, M. Jonas, E.R. Edelman, C.L. Feldman, P.H. Stone, Role of endothelial shear stress in the natural history of coronary atherosclerosis and vascular remodeling: molecular, cellular, and vascular behavior, J. Am. Coll. Cardiol. 49 (25) (2007) 2379–2393.
[55] S. Reakasame, A.R. Boccaccini, Oxidized alginate-based hydrogels for tissue engineering applications: a review, Biomacromolecules 19 (1) (2017) 3–21.
[56] V. Mohamed-Ali, J. Pinkney, S. Coppack, Adipose tissue as an endocrine and paracrine organ, Int. J. Obes. 22 (12) (1998) 1145.
[57] Y. Deng, P.E. Scherer, Adipokines as novel biomarkers and regulators of the metabolic syndrome, Ann. N. Y. Acad. Sci. 1212 (2010) E1.
[58] F. Stillaert, M. Findlay, J. Palmer, R. Idrizi, S. Cheang, A. Messina, K. Abberton, W. Morrison, E.W. Thompson, Host rather than graft origin of Matrigel-induced adipose tissue in the murine tissue-engineering chamber, Tissue Eng. 13 (9) (2007) 2291–2300.
[59] L. Wu, T. Wang, Y. Ge, X. Cai, J. Wang, Y. Lin, Secreted factors from adipose tissue increase adipogenic differentiation of mesenchymal stem cells, Cell Prolif 45 (4) (2012) 311–319.